Solar-assisted adsorption cycle for the production of cooling effect and potable water

Kim Choon NG[1], Kyaw Thu[2] and Young Deuk Kim[2]

[1]National University of Singapore, Department of Mechanical Engineering
9 Engineering Drive 1, Singapore 117576, Singapore,
Visiting Professor, WDRC, KAUST, Saudi Arabia.

[2]King Abdullah University of Science and Technology, Water Desalination and Reuse Center
Thuwal 23955-6900, Saudi Arabia

Abstract

Is there a practical thermodynamic cycle for desalination that operates at specific energy consumption close to the thermodynamic limit? If yes, by how much higher would it be? The conventional desalination processes such as the Multi-stage flash (MSF), the Multi-effect distillation (MED), the Reverse Osmosis (RO), etc., have energy consumption levels exceeding the thermodynamic limit (typically at 0.78 kWh/m^3) by as much as 5 to 12 times. It has been reported that the present challenge in energy efficiency for the desalination industry is to have an amicable specific energy consumption of 1.5 kWh/m^3.

In this paper, an efficient adsorption (AD) cycle for desalination is presented that employs only waste heat, typically at 55° to 85°C. With only a single thermal input, the AD cycle produces two useful effects, namely the high-grade water and cooling capacity suitable for air-conditioning. Low-temperature waste heat, such as solar thermal or exhaust of industrial processes, is available readily in abundance either from industrial processes or the solar thermal and it is essentially free. This is because if not recovered, the waste heat would be purged into the ambient. We present our patented adsorption desalination cycle, the simulation and the experimentally measured performance data of an AD prototype, housed in the laboratory of NUS. The performances cover over a wide range of operating conditions such as heat source, cooling and chilled water temperatures. The measured data are succinctly summarized in terms of key parameters such as the specific daily water production (SDWP) and the specific cooling capacity (SCP) which are suitable for design purposes. The adsorbent-adsorbate pair used in the cycle is the silica gel-water pair which is environment-friendly, and the estimated electricity consumption of AD cycle is only 1.38 kWh/m^3; – the lowest specific energy consumption ever reported for desalination. With almost no major moving parts, the AD cycle has low maintenance. Based on a life-cycle costing, the water production cost from a large-scale AD plant is estimated at US$0.457/m^3 which is, hitherto, the lowest in comparison to all other desalination methods.

Keywords

Desalination, cooling, waste heat recovery, potable water cost, solar hot water system

Introduction

Potable water is basic and essential resource for supporting human lives and economic activities. Almost all our daily needs such as food, drinking water and amenities etc., relate to the water usage directly or indirectly. Although water supply in many countries is influenced by rainfall and climatic changes, but the increasing demands for fresh water has outstripped the supply from natural sources such as rainfall, rivers, ground water, etc. Such demands for water are from the domestic, industrial and agricultural sectors have dominate the water supply patterns of an economy[1]. In the agriculture sector, a large amount of water is needed for food production; For example, 24 m^3 of water is used to produce 1 kg of chocolate, 15.5 m^3 for 1 kg of beef and up to 4m^3 is needed for 1 litre of biofuels [2]. Water utilization in the agriculture sector is known to be the highest despite much effort in improving the efficiency and the switch to more efficient production methods. Global water shortage of an economy is compounded by rapid population increase as well as the climatic changes that resulted from global warming, etc. Natural occurring fresh or potable water on Earth constitutes less than 1% of the available water resources, whilst 97% of the water is saline water, found mostly in the oceans. Of the 1% fresh water available, a majority of the water is locked in forms not convenient to be extracted such as the ice-caps or deposited deep under the ground. Moreover, the water consumption of many countries is expected to double every 10 to 20 years, almost twice that of the population growth rate [3].

Desalination is a process of removing dissolved salts from sea or brackish water and it is a practical solution for quenching global thirst[4]. With technological advancement in desalination methods, more than 40 million cubic meter per day of water are produced by three generic methods, namely (1) boiling and condensation, (2) separation by filtration through membrane and (3) separation by electro-chemical reaction [5-10]. Although membranes are becoming widely used in the world, thermally-driven methods are dominantly used in the Middle East region.

Cost of Desalination

The unit production cost of water production is the key indicator for evaluating the efficacy of a desalination method. Desalination cost is the sum of capital and operation costs [11-14]. Capital cost is determined by the life-span of equipment and the interest rates for the amortisation of borrowed capital. The operation cost includes the energy cost, maintenance cost, chemicals, as well as the pre- and post-treatment costs. When high-grade energy sources are used in these processes, such as high temperature steam or electrical energy, the cost analysis is easily determined. However, when renewable or waste heat is used in the desalination processes, only the electricity consumed by the plant is considered payable and the recovered waste heat is deemed as “free or non-payable”[15]. Examples of desalination plants that utilize the combined low and high grade energy input are the multi-effect distillation (LT-MED), membrane distillation (MD) and more recently, the adsorption desalination (AD) [16, 17]. Another example of “non-payable” energy input is the natural evaporation of seawater by the heating from the sun. The water vapour rises from the seas and rivers to a higher elevation where precipitation could occur in the cooler air. Based on an annual average rainfall of about 990 mm, the specific energy consumption of the naturally occurring rain water is determined at 475 kWh/m^3. The rainwater runoff is collected at rivers or dams and then treated for chloride and other salts that are beneficial to human consumption. For simplicity, the energy needed for desalting brackish or sea water is classified into payable and non-payable (or free) portions. Engineers and scientists could design desalination cycles, e.g., the adsorption desalination cycles, where the consumption of the non-payable energy in the desalination processes could be enhanced.

In this paper, we propose a method of evaluating the efficacy of a desalination plant with a parameter that could track both the total primary energy (*TPE*) consumption and the payable energy (PPE). The *TPE* is the summation of all required energy to produce 1 m^3 of potable water by a desalination method and it is given as:

$$TPE_{\delta=1}^{\beta=1} \text{ or } PPE_{\delta=0}^{\beta=1} = \sum\left(\frac{E_{Thermal}}{\eta_b}\delta + \frac{E_{Elc}}{\eta_c}\beta\right) \qquad (1)$$

where $E_{Thermal}$ and E_{Elec} are the unit energy consumption by thermal and electricity, respectively, whilst η_b (= 0.8) and η_c (= 0.45) are the efficiencies of the boiler and the power grid. The multipliers δ and β are integers with their values of 1 or 0 depending if they are taken to be TPE or PPE. The generic unit cost of desalination can now be applied to all types of desalination plants, including the naturally occurring rain water of the hydrology cycle with solar input. The existing desalination systems such as MSF, MED, MD, AD and RO processes that incur both thermal and electric energy can also be accounted for with TPE and PPE. Fig. 1 gives the cost comparison for the major desalination processes and their energy consumption are compared with the thermodynamic limit of 0.78 kWh/m^3.

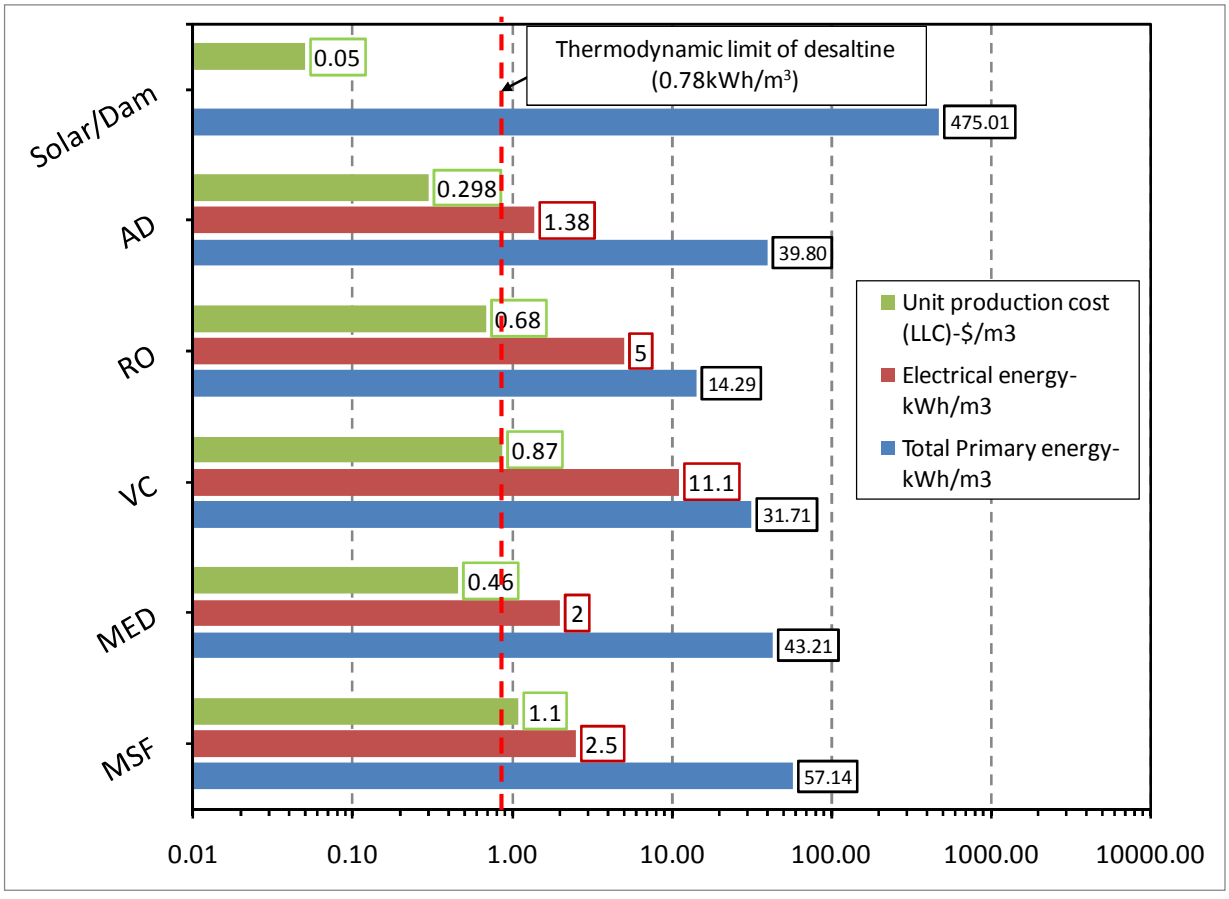

Fig. 1 The energy and cost map of desalination technologies

In the case of water from rainfall, the total solar energy input to evaporate seawater can be computed with the assumptions of (i) an annual average rainfall of 990 mm [18-20] and (ii) an efficiency of 30% of the average irradiance of 174 W/m^2, and this yields a TPE of 475 kWh/m^3, which is deemed inefficient in comparison with the thermodynamic limit. However,

the fresh water from rainfall has zero cost. Should the thermal energy consumed in the desalting process is unused, it would have been purged or lost into the ambient. More recent development in low temperature multi-effect distillation (LT-MED) and adsorption desalination (AD) systems can now be compared with other conventional desalination plants can now be compared fairly by using the concept of TPE and PPE. Low temperature waste heat, typically less than 85 °C, is extracted from exhaust of industrial processes or the renewable sources which are deemed free. Only the capital cost for the energy extraction apparatus such as heat exchangers are to be duly considered in the unit cost computation [22].

Adsorption and Adsorption Desalination and Cooling

Adsorption is the adhesion or accumulation of atoms, ions, biomolecules or molecules of gas, liquid, or dissolved solids to the interfacial layer of a porous substance[23]. The term "adsorption" is first introduced by Kayser in 1881 to describe his observation of the condensation of gases on free surfaces [24] and it occurs whenever a solid surface is exposed to a gas or liquid: It is defined as the enrichment of material or increase in the density of the fluid in the vicinity of an interface [25]. When a porous surface is heated, the previously trapped molecules are released from the force field and this process is termed desorption.

The authors have designed cyclic processes to exploit the sorption phenomena and they have patented cycles for the production of cooling and water [26-29]. They employ the silica gel (pore surface area > 720 m^2/g) and water as the working pair, where saline solution is first exposed to the un-saturated adsorbent over a half cycle interval. Concomitantly, the previously saturated adsorbent is simultaneously heated by a low temperature heat source, driving off the trapped water vapour and pushing the vapour to condense on tubes surfaces which are cooled by circulating water from either a closed or open-type cooling tower. Details of the adsorption chillers and desalination cycles can be found widely in the literature. The salient advantages of the AD cycle over the other desalination cycles are (i) it can be powered by a low temperature heat source, (ii) it has almost no major moving parts, (iii) and it has low maintenance and (iv) it is environment friendly. A schematic of the adsorption chiller and desalination cycle is shown in Fig.2. Type RD silica gel is selected as the adsorbent and its thermo-physical properties are listed in Table 1. Sea or brackish water is de-aerated prior to feeding into the evaporator. Evaporation is initiated instantaneously by the vapour uptake to the adsorbent (silica gel), thereby removing the dissolved salts in the solution. Desorbed vapour is condensed in a condenser unit and it is essentially a high-grade potable water where the total dissolved solids (TDS) are less than 10ppm.

Modelling of solar-assisted adsorption desalination cycles

The solar-assisted adsorption desalination cycle includes two sections; the solar hot water production system and the adsorption desalination system. The monthly average hourly global irradiance incident upon a tilted surface is estimated based on the meteorological data obtained from Singapore Meteorological Service (SMS) for the period of 1988-1997. The global irradiance consists of beam and diffuse components. The extraterrestrial radiation incident on a horizontal surface at any time between sunrise and sunset is calculated using the following equation [30]:

$$G_o = G_{sc}\left(1+0.033\cos\frac{365n}{365}\right)\cos\theta_z \qquad (2)$$

where the solar constant, G_{sc}, is equal to 1367 W/m^2 (Iqbal, 1983) and n is the day of the year. The value of G_o depends on geographic latitude as well as time of day and year. The values of solar zenith angle (θ_z) are calculated as:

$$\cos\theta_z = \cos\phi\cos\delta\cos\omega + \sin\phi\sin\delta \quad (3)$$

where the declination δ is determined by (Cooper, 1969):

$$\delta = 23.45\sin\left(360\frac{284+n}{365}\right) \quad (4)$$

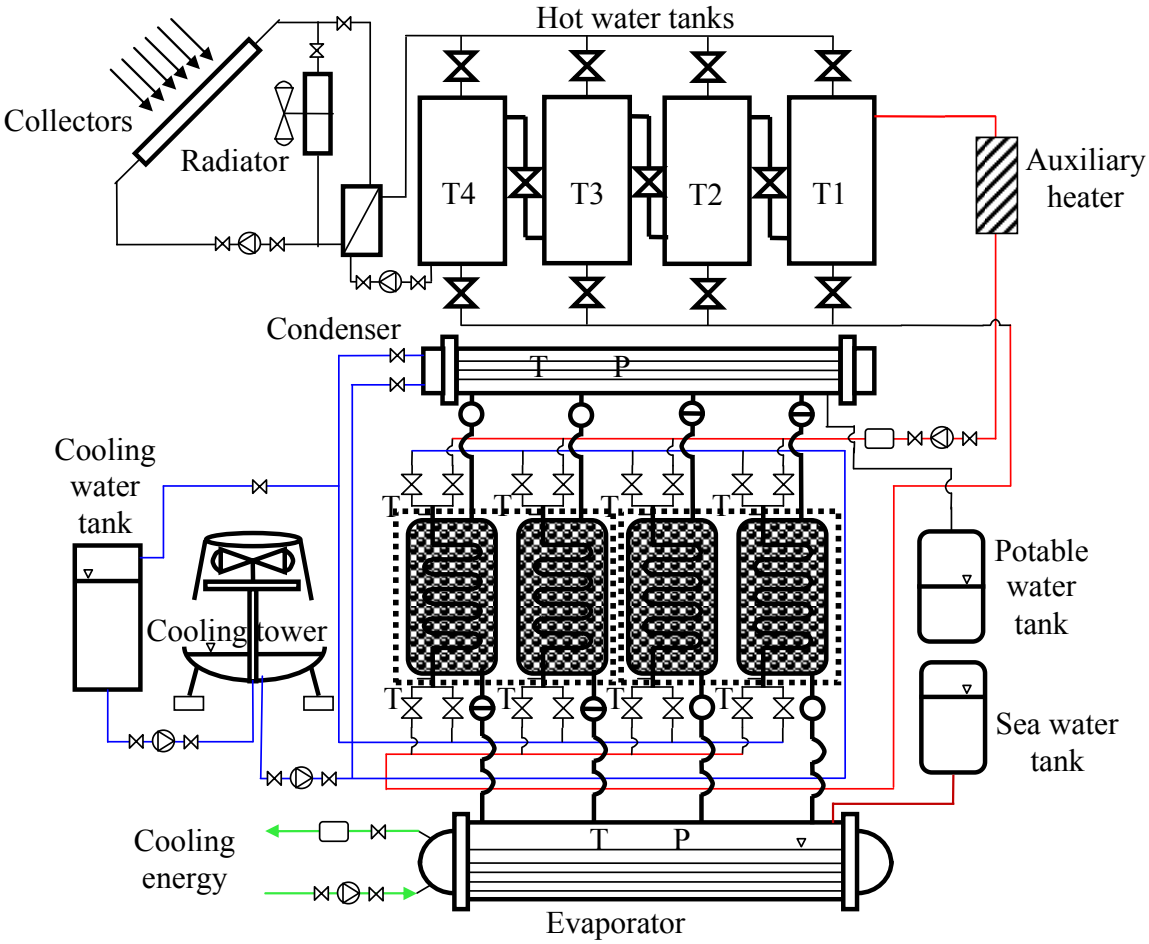

Fig. 2 The description of the solar-assisted adsorption desalination cum cooling cycle

Property	Value
Pore size (nm)	0.8-7.5
Porous volume (cm^3/g)	0.37
Surface area (m^2/g)	720
Average pore diameter (nm)	2.2
Apparent density (kg/m^{-3})	700
pH (-)	4.0
Specific heat capacity (kJ/kg·K)	0.924
Thermal conductivity (W/m·K)	0.198

Table 1. Thermo-physical properties of Type RD silica gel

In order to evaluate the hour angle in Eq. (3), local time is converted to solar time using two corrections. The first correction takes into account the difference between the locations of the meteorological station (Changi International Airport, 1° 37′ N, 103° 98′ E) and the meridian on

which local standard time is based. The second correction adjusts for the perturbations in the earth's rate of rotation and is expressed in terms of the equation of time. For a location east to the Greenwich meridian, solar time is given as,

$$\text{solar time} = \text{standard time} + 4\left(L_{st} - L_{loc}\right) + E \tag{5}$$

where the equation of time E is given by [31]:

$$E = 229.2\left(0.000075 + 0.001868\cos B - 0.032077\sin B - 0.014615\cos 2B - 0.04089\sin 2B\right) \tag{6}$$

with

$$B = (n-1)\frac{360}{365} \tag{7}$$

The daily extraterrestrial radiation is obtained by integrating Eq. (2) over the period from sunrise to sunset and the equation is

$$H_o = \frac{24\times 3600 G_{sc}}{\pi}\left(1 + 0.033\cos\frac{365n}{365}\right)\left(\cos\phi\cos\delta\sin\omega_s + \frac{\pi\omega_s}{180}\sin\phi\sin\delta\right) \tag{8}$$

where the sunset angle ω_s is

$$\omega_s = \cos^{-1}\left(-\tan\phi\tan\delta\right) \tag{9}$$

The monthly average daily extraterrestrial radiation, H_o, can be calculated using n and δ for the mean day of the month. To obtain the monthly average daily diffuse and beam radiation from the measured monthly average daily global radiation, the monthly average daily diffuse radiation H_d is calculated from monthly average diffuse fraction correlation [32]:

$$\frac{H_d}{H_h} = 0.775 + 0.347\left(\omega_s - 90°\right)\frac{\pi}{180°} - \left[0.505 + 0.261\left(\omega_s - 90°\right)\frac{\pi}{180°}\right]\cos\left[\frac{180°}{\pi}\left(K_T - 0.9\right)\right] \tag{10}$$

where the monthly average clearness index K_T is the ratio of monthly average daily radiation on a horizontal surface to the monthly average daily extraterrestrial radiation

$$K_T = \frac{H_h}{H_o} \tag{11}$$

Then, the monthly average daily diffuse and global radiations, H_d and H_h, are converted into the monthly average hourly diffuse and global radiations, I_d and I_h, by means of the ratio of hourly global to daily global radiation, as a function of day length and the hour in question (32, 33

$$I_d = r_d\left(\omega, \omega_s\right)H_d \tag{12}$$

$$I_h = r_h\left(\omega, \omega_s\right)H_h \tag{13}$$

where

$$r_d\left(\omega, \omega_s\right) = \frac{\pi}{\tau_{\text{day}}}\frac{\cos\omega - \cos\omega_s}{\sin\omega_s - \frac{\pi\omega_s}{180°}\cos\omega_s} \tag{14}$$

$$r_h\left(\omega, \omega_s\right) = \left(a + b\cos\omega\right)r_d\left(\omega, \omega_s\right) \tag{15}$$

In these equations τ_{day} = 24 h, and the hour angle

$$\omega = \frac{360°}{\tau_{\text{day}}}t \tag{16}$$

represents the time of day t, while the time of year enters only through the sunset hour angle ω_s

$$\cos\omega_s = -\tan\phi\tan\delta \tag{17}$$

The coefficients a and b are given by

$$a = 0.4090 + 0.5016\sin\left(\omega_s - 60°\right) \tag{18}$$

$$b = 0.6609 - 0.4767\sin\left(\omega_s - 60°\right) \tag{19}$$

The isotropic diffuse model is conservative, i.e., it tends to underestimate I_t, and makes calculation of radiation on tilted surfaces easy. However, improved models have been developed which take into account the circumsolar diffuse and horizon brightening components on a tilted surface. Hay and Davies (1980) estimated the fraction of the diffuse that is circumsolar and consider it to be all from the same direction as the beam radiation, but they do not consider horizon brightening [34]. Temps and Coulson (1977) account for horizon brightening on clear days by applying a correction factor of $\left[1+\sin^3(\beta/2)\right]$ to the isotropic diffuse [35]. Klucher (1979) modified this correction factor by a modulating factor f so that is has the form $\left[1+f\sin^3(\beta/2)\right]$ to account for cloudiness [36]. Reindl et al. (1990) have modified the Hay and Davies [1980] model by the addition of a term like that of Klucher (1979), giving a model to be referred to as the Hay-Davies-Klucher-Reindl (HDKR) diffuse model. The diffuse on the tilted surface is

$$I_{d,t} = I_d\left\{\left(1-A_i\right)\left(\frac{1+\cos\beta}{2}\right)\left[1+f\sin^3\left(\frac{\beta}{2}\right)\right]+A_iR_b\right\} \tag{20}$$

where A_i is an anisotropic index which is a function of the transmittance of the atmosphere for beam radiation

$$A_i = \frac{I_{bn}}{I_{on}} = \frac{I_b}{I_o} \tag{21}$$

and

$$f = \sqrt{I_b / I_h} \tag{22}$$

The total radiation on the tilted surface is then

$$I_T = \left(I_b + I_dA_i\right)R_b + I_d\left(1-A_i\right)\left(\frac{1+\cos\beta}{2}\right)\left[1+f\sin^3\left(\frac{\beta}{2}\right)\right]+I_h\rho_g\left(\frac{1-\cos\beta}{2}\right) \tag{23}$$

where the geometric factor R_b, the ratio of beam radiation on the tilted surface to that on a horizontal surface at any time, is given by

$$R_b = \frac{I_{b,t}}{I_b} = \frac{\cos\theta_i}{\cos\theta_z} \tag{24}$$

and $\cos\theta_i$ is determined from

$$\begin{aligned}\cos\theta_i = {} & \sin\delta\sin\phi\cos\beta - \sin\delta\cos\phi\sin\beta\cos\gamma + \\ & \cos\delta\cos\phi\cos\beta\cos\omega + \cos\delta\sin\phi\sin\beta\cos\gamma\cos\omega + \cos\delta\sin\beta\sin\gamma\sin\omega\end{aligned} \tag{25}$$

In Eq. (20) the extraterrestrial radiation I_o on a horizontal surface for an hour period is obtained by integrating Eq. (1) for a period between hour angles ω_1 and ω_2 which define an hour

$$I_o = \frac{12\times 3600G_{sc}}{\pi}\left(1+0.033\cos\frac{365n}{365}\right)\left(\cos\phi\cos\delta\left(\sin\omega_2-\sin\omega_1\right)+\frac{\pi\left(\sin\omega_2-\sin\omega_1\right)}{180}\sin\phi\sin\delta\right) \tag{26}$$

The calculation of absorbed radiation using the HDKR model of diffuse radiation is similar to that based on the isotropic model except that the circumsolar diffuse is treated as an increment to the beam radiation, horizon brightening is considered, and the diffuse component is correspondingly reduced.

The collector efficiency is defined as the ratio between the useful energy delivered over the aperture area and the total irradiance of the collector aperture, according to [37]:

$$\eta = \frac{q_u}{A_aG_T} = \frac{\dot{m}_pc_{p,c}\left(T_{c,o}-T_{c,i}\right)}{N_cA_aG_T} \tag{27}$$

The efficiency curve provided by manufacturer is obtained from efficiency tests according to the standard (EN 12975-2:2006). The efficiency curve is described after a second degree fit of efficiency points measured at different collector temperatures and follows from:

$$\eta = \eta_0 - c_1 \frac{T_m - T_a}{G_T} - c_2 G_T \left(\frac{T_m - T_a}{G_T} \right)^2 \quad (28)$$

with $T_m = \frac{T_{c,i} + T_{c,o}}{2}$.

Since the efficiency curve is produced on the basis of normal incidence measurements, its use for different incident angles requires the correction of the optical efficiency, measured at normal incidence, by the appropriate incident angle modifier. Thus, the collector efficiency at any incidence angle is calculated as:

$$\eta(\theta) = \eta_0 K(\theta) - c_1 \frac{T_m - T_a}{G_T} - c_2 G_T \left(\frac{T_m - T_a}{G_T} \right)^2 \quad (29)$$

where the incidence angle modifier $K(\theta)$ can be approximated by the product of the transversal and longitudinal incidence angle modifiers according to [38]:

$$K(\theta) \equiv K\left(\theta_l, \theta_t\right) \approx K\left(\theta_l, 0\right) K\left(0, \theta_t\right) \quad (30)$$

From Eqs. (26) and (28), the collector outlet temperature is calculated using following equation:

$$\frac{q_u}{A_a} = \eta_0 K(\theta) G_T - c_1 \left(T_m - T_a\right) - c_2 \left(T_m - T_a\right)^2 - c_3 \frac{dT_m}{dt} \quad (31)$$

For the four storage tanks, it is noted that the hot water mass flow rate withdrawn from the storage tank 1 in the SHWP is equal to the desired load flow rate, regardless of storage temperature. On the other hand, whenever the storage tank 1 temperature falls below the desired load temperature, the maximum possible portions of the energy demand is met by keeping the discharge mass flow rate equals to the desired load flow rate and the rest of the energy demand is supplied by the auxiliary.

A control function F_i^c that determines to which storage tank receives water from the heat exchanger is written as follows:

$$F_i^c = \begin{cases} 1 \text{ if } T_{h,o} > T_{t,i}, i = 1 \\ 1 \text{ if } T_{t,i-1} \geq T_{h,o} > T_{t,i} \\ 1 \text{ if } T_{h,o} < T_{t,i}, i = 4 \\ 0 \text{ otherwise} \end{cases} \quad (32)$$

The water returning from the load is controlled in a similar manner with a load return control function F_i^l:

$$F_i^l = \begin{cases} 1 \text{ if } T_r > T_{t,i}, i = 1 \\ 1 \text{ if } T_{t,i-1} \geq T_r > T_{t,i} \\ 1 \text{ if } T_r < T_{t,i}, i = 4 \\ 0 \text{ otherwise} \end{cases} \quad (33)$$

The net flow between storage tanks depends on the magnitudes of the collector and flow rates and the values of the two control functions at any particular instant, and a mixed-flow rate that represents the net flow into tank *i* from tank *i*-1:

$$F_i' = \begin{cases} \dot{m}_{m,1} = 0 \\ \dot{m}_{m,i} = \dot{m}_c \sum_{j=1}^{i-1} F_j^c - \dot{m}_l \sum_{j=i+1}^{N} F_j^l \\ \dot{m}_{m,N+1} = 0 \end{cases} \quad (34)$$

With these control functions, energy balance of a well-mixed storage tank i can be expressed as

$$m_i c_{p,t,i} \frac{dT_{t,i}}{dt} = (UA)_i \left(T_a - T_{t,i}\right) + F_i^c \dot{m}_c \left(c_{p,h} T_{h,o} - c_{p,t,i} T_{t,i}\right) + \begin{cases} F_i^l \dot{m}_l \left(c_{p,r} T_r - c_{p,t,i} T_{t,i-1}\right) \text{ if } F_k^c = F_i^l = 1 \text{ with } k < i \\ F_i^l \dot{m}_l \left(c_{p,r} T_r - c_{p,t,i} T_{t,i}\right) \end{cases} + \begin{cases} \dot{m}_{m,i} \left(c_{p,t,i-1} T_{t,i-1} - c_{p,t,i} T_{t,i}\right) \text{ if } \dot{m}_{m,i} > 0 \\ \dot{m}_{m,i+1} \left(c_{p,t,i} T_{t,i} - c_{p,t,i+1} T_{t,i+1}\right) \text{ if } \dot{m}_{m,i+1} < 0 \\ F_{i+1}^l \dot{m}_l \left(c_{p,t,i+1} T_{t,i+1} - c_{p,t,i} T_{t,i}\right) \text{ if } F_k^c = F_{i+1}^l = 1 \text{ with } k \geq i+1 \end{cases} \quad (35)$$

Energy demand met by the solar energy is calculated as,

$$q_s = \dot{m}_l c_{p,sa} \left(T_s - T_a\right) \quad (36)$$

When $T_s < T_l$, the desired load temperature requirement can be met by an auxiliary energy. The required auxiliary energy is calculated as,

$$q_a = \dot{m}_l c_{p,ls} \left(T_l - T_s\right) \quad (37)$$

The present mathematical modeling of a solar assisted 2-bed advanced adsorption desalination cycle with the heat recovery between the condenser and the evaporator is developed based on adsorption isotherms, adsorption kinetics and energy balances between the sorption elements (adsorber/desorber heat exchangers), the evaporator and the condenser. Dubinin–Astakhov (D-A) equation is used for the calculation of the water vapour uptake by the silica gel at specific temperature and pressure and is given by,

$$q^* = q_0 \exp\left[-\left(\frac{RT}{E} \ln\left(\frac{P}{P_0}\right)\right)^n\right] \quad (38)$$

where, q_0 is the maximum adsorbed amount, E is the characteristic energy and n is the surface heterogeneity parameter. The transient uptake of by the silica gel can be obtained by linear driving force equation as,

$$\frac{dq}{dt} = \frac{15 D_{s0} \exp\left(\frac{-E_a}{RT}\right)}{R_p^{\,2}} \left(q^* - q\right) \quad (39)$$

where R_p denotes the average radius of a silica gel particle, E_a is the activation energy of surface diffusion, and D_{so} is the kinetic constant for the silica gel water system.

It is assumed that the adsorbed and desorbed amounts of water vapour during the adsorption and desorption are the same and the overall mass balance of the cycle is given by,

$$\frac{dM_{s,evap}}{dt} = \dot{m}_{s,in} - \dot{m}_{d,cond} - \dot{m}_b \tag{40}$$

Here, $M_{s,evap}$ is the amount of sea water in the evaporator, $\dot{m}_{s,in}$ is the rate of feed sea water, $\dot{m}_{d,cond}$ is the mass of potable water extracted from the condenser and $\dot{m}_b$ is the mass of concentrated brine rejected from the evaporator. The energy balance of the evaporator in communication with the adsorbers is written as,

$$\begin{aligned}&\left[c_{p,s}\left(T_{evap}\right)M_{s,evap} + M_{HX,Evap}\ c_{pHX}\right]\frac{dT_{evap}}{dt} = h_f\left(T_{evap}\right)\dot{m}_{s,in} - \\ &h_{fg}\left(T_{evap}\right)M_{sg}\left(\frac{dq_{ads}}{dt}\right) + \dot{m}_{evap}\ c_{p,evap}\left(T_{chilled,in} - T_{chilled,out}\right)\end{aligned} \tag{41}$$

Similarly, the energy balance of the condenser is given by,

$$\begin{aligned}&\left[c_p\left(T_{cond}\right)M_{cond} + M_{HX,Cond}\ c_{pHX}\right]\frac{dT_{cond}}{dt} \\ &= -h_f\left(T_{cond}\right)\frac{dM_d}{dt} + h_{fg}\left(T_{cond}\right)M_{sg}\left(\frac{dq_{des}}{dt}\right) \\ &+ \dot{m}_{cond}c_{p,cond}\left(T_{cond,in} - T_{cond,out}\right)\end{aligned} \tag{42}$$

In this cycle, $\dot{m}_{cond} = \dot{m}_{evap}$ since water re-circulating circuit is employed across the evaporator and the condenser for heat recovery. The energy balance of the adsorber/desorber is given by,

$$\begin{aligned}&\left(M_{sg}c_{p,sg} + M_{HX,Ads}c_{p,HX} + M_{abe}c_{p,a}\right)\frac{dT_{ads/des}}{dt} = \pm Q_{st}\left(T_{ads/des}, P_{evap/cond}\right) \\ &n \times M_{sg}\frac{dq_{ads/des}}{dt} \pm \dot{m}_{cw/hw}\ c_{p,cw/hw}\left(T_{ads/des}\right)\left(T_{cw/hw,in} - T_{cw/hw,out}\right)\end{aligned} \tag{43}$$

where n is the number of adsorber or desorber bed in the cycle. In this analysis, the value of n is 2 since a pair of two reactors is under adsorption process whilst the other pair is under desorption mode. The specific heat capacity c_p is calculated as a function of adsorber temperature (T_{ads}) or desorber temperature (T_{des}) during adsorption or desorption process, respectively. Here Q_{st} stands for the isosteric heat of adsorption which is calculated [39, 40] as follow,

$$Q_{st} = h_{fg} + E\left\{-\ln\left(\frac{q}{q_m}\right)\right\}^{1/n} + Tv_g\left(\frac{\partial P}{\partial T}\right)_g \tag{44}$$

where v_g is the specific volume of the gaseous phase, h_{fg} is the latent heat.

The outlet temperature of the water from each heat exchanger is estimated using log mean temperature difference method and it is given by,

$$T_{out} = T_0 + \left(T_{in} - T_0\right)\exp\left(\frac{-UA}{\dot{m}c_p\left(T_0\right)}\right) \tag{45}$$

Here T_0 is the temperature of the heat exchanger assuming uniform temperature across the reactor heat exchanger. In the advanced AD cycle where the heat recovery between the evaporator and the condenser is achieved by the heat recovery loop that circulates the water in between them. In this case, the outlet water from the evaporator is channelled to the inlet of the condenser whilst the outlet water from the condenser is sent to the evaporator.
The energy required to remove water vapors from the silica gels, (Q_{des}), can be calculated by using the inlet and outlet temperatures of the heat source supplied to the reactors, and this is given by,

$$Q_{des} = \dot{m}_{hw} c_{p,hw}(T_{hw})\left(T_{hw,in} - T_{hw,out}\right) \tag{46}$$

where $\dot{m}_{hw}$ indicates the mass flow rate and $c_{p,hw}$ defines the specific heat capacity of heating fluid. Concomitantly, the energy rejected to the cooling water during the adsorption process is estimated by the inlet and outlet temperatures of cooling fluid supplied to the other reactor and this is written as,

$$Q_{ads} = \dot{m}_{cw} c_{p,cw}(T_{cw})\left(T_{cw,out} - T_{cw,in}\right) \tag{47}$$

where $\dot{m}_{cw}$ and $c_{p,cw}$ indicate the mass flow rate and the specific heat capacity of cooling fluid. At the same time, the heat of evaporation (Q_{evap}), and the condensation energy (Q_{cond}) rejected at the condenser are given by,

$$Q_{evap} = \dot{m}_{evap} c_{p,evap}(T_{evap})\left(T_{chilled,in} - T_{chilled,out}\right) \tag{48}$$

$$Q_{cond} = \dot{m}_{cond} c_{p,cw}(T_{cond})\left(T_{cond,out} - T_{cond,in}\right) \tag{49}$$

It is noted that the roles of the reactors for adsorption or desorption are switched in a half-cycle time.

The SDWP and SCP of the cycle is defined as,

$$SDWP = \int_0^{t_{cycle}} \frac{Q_{cond}\tau}{h_{fg}\left(T_{cond}\right) M_{sg}} dt \tag{50}$$

$$SCP = \int_0^{t_{cycle}} \frac{Q_{evap}\tau}{M_{sg}} dt \tag{51}$$

The performance ratio (PR) for desalting and the coefficient of performance (COP) of the adsorption cycle are given as,

$$PR = \int_0^{t_{cycle}} \frac{\dot{m}_{water} h_{fg}\left(T_{cond}\right)\tau}{Q_{Mdes} + Q_{Sdes}} dt \tag{52}$$

$$COP = \int_0^{t_{cycle}} \frac{Q_{evap}\tau}{Q_{Mdes} + Q_{Sdes}} dt \tag{53}$$

Finally, the overall performance of the adsorption cycle which produces two useful effects (cooling energy and potable water) from a single heat input i.e., the low temperature waste heat is analyzed using overall conversion ratio (OCR). The OCR is defined as the ratio of the total useful effects produced over the energy input, and the expression is given as,

$$OCR = \int_{0}^{t_{cycle}} \frac{\left(Q_{evap} + Q_{cond}\right)\tau}{Q_{Mdes} + Q_{Sdes}} dt \qquad (54)$$

The mathematical modeling equations of the adsorption desalination cum cooling cycle are solved using the Gear's BDF method from the IMSL library linked by the simulation code written in FORTRAN PowerStation, and the solver employs a double precision with tolerance value of $1x10^{-8}$.

Result and discussion

The production of dual useful effects; namely cooling and potable water, are investigated for two operating conditions: In the first operating states, the cycle is operated to produce high-grade cooling power i.e., the temperature of the chilled water outlet is 7 to 9°C for the residential or space cooling by maintaining the chilled water inlet to the evaporator around 12-14°C. In the second condition, the operation is optimized for the production of potable water with the increase in chilled water inlet temperature to 25-30°C. The outlet chilled water temperature which is around 20-25°C can be used for process cooling. It is noted that in both operating conditions, the cycle produces the cooling power and potable water simultaneously.
Fig. 3 gives the five day-temperature profiles of the hot water storage tanks for the month of July. The lowest temperature of the tank #1 in the late night hour is about 54.8 °C whilst the highest temperature is about 86.65 °C.

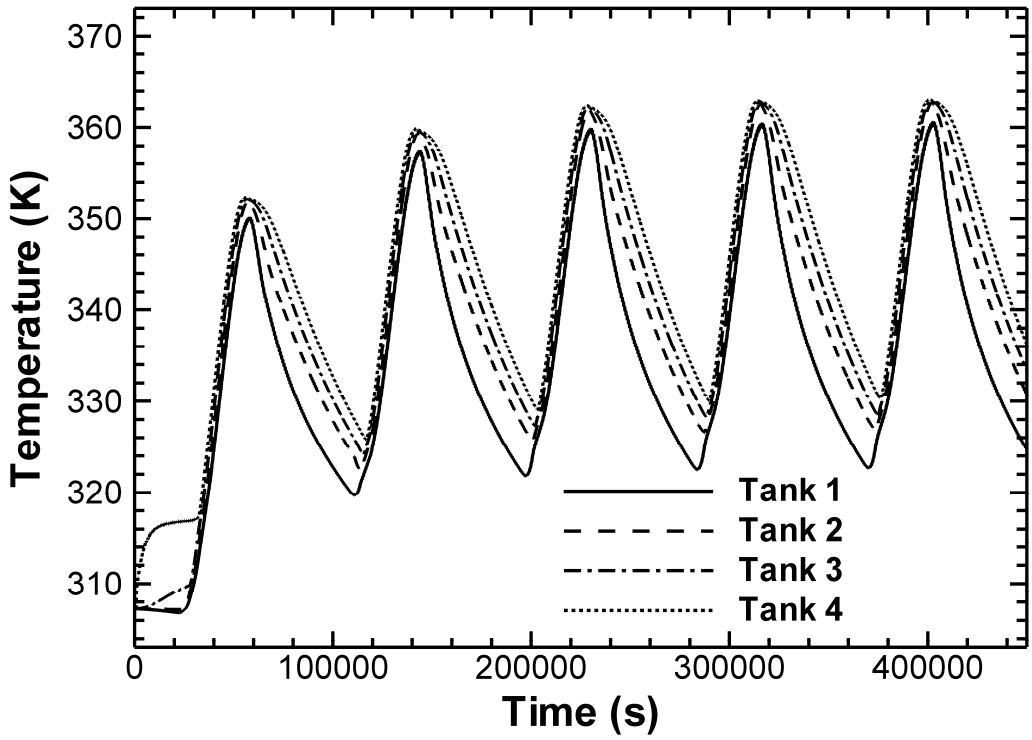

Figure 3 Temperature profiles of the storage tank for five consecutive days in July

At solar noon, the temperature difference between tank#1 and tank#2 is around 0.2 ˚C whilst that in the mid-night hours is around 2 ˚C. Good temperature stratification is incorporated in the plant by having a top-to-bottom arrangement for the storage tanks and the temperature-controlled filling of water from the solar collector. Fig. 4 shows the performance of the adsorption desalination cum cooling cycle that operates using hot water produced from the solar hot water system. It is observed that the temperature of the evaporator is influenced by the hot water supply temperature. At solar noon, the hot water temperature increases up to 86.65 ˚C and the evaporator temperature is about 20 ˚C while the chilled water inlet temperature is set at 30 ˚C.

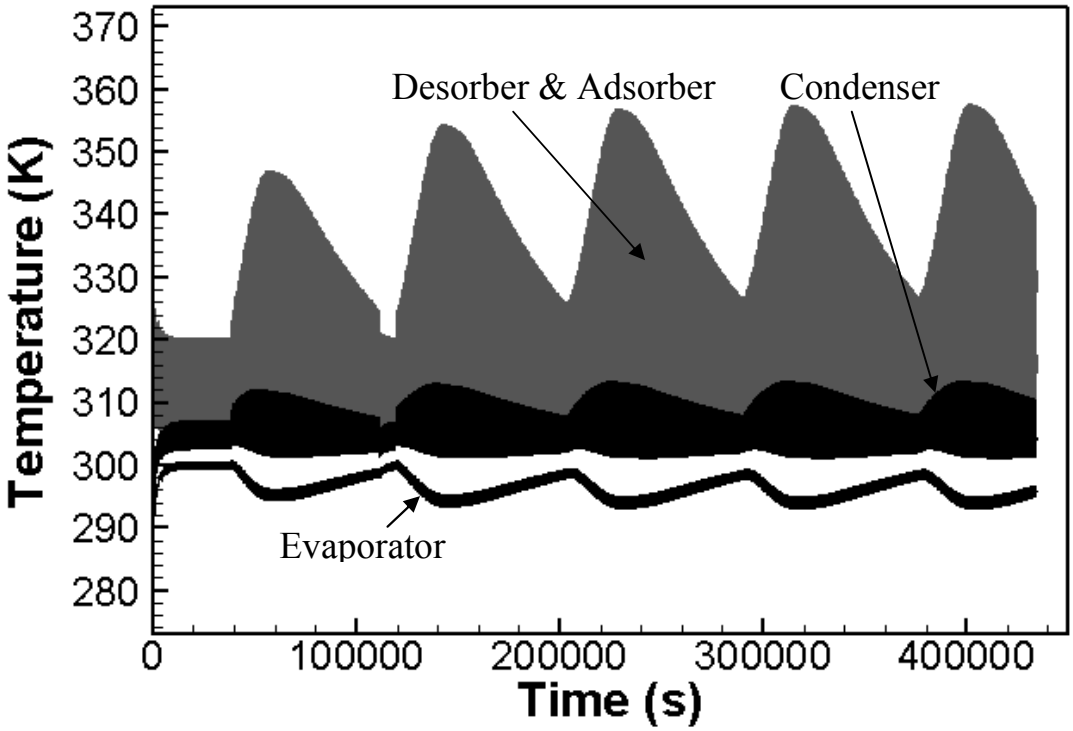

Fig. 4 The temperature profile of the solar-assisted adsorption desalination cum cooling cycle

A simulation of the performance of prototype AD plant is given Fig. 5 where the cyclic steady state performance of the adsorber, the desorber, the condenser and the evaporator are depicted. Over the day, the desorber bed temperature first rises with increasing solar radiation before noon and then dropping gradually in the after noon as the solar irradiance reduces. The condenser and the adsorber temperatures remain relatively constant since the external cooling water circuits are used for the heat rejection.

The simulations are compared with experiments using a prototype test facility at the air-conditioning laboratory of National University of Singapore. A pictorial view of the experimental AD plant is shown in Fig. 6. The plant consists of four major components: (i) Adsorber beds, (ii) Desorber beds, (iii) an evaporator and (iv) a condenser. As the plant is fully automated, it can be configured to operate either as a 2-bed or 4-bed mode as well as with or without the energy recovery schemes during the switching intervals. The latter schemes are invoked so as to improve the COP of the plant. Table 2 lists the parameters of the components in the pilot plant. From such a facility, a dearth of experimental data have been gathered for a wide range of operating conditions, namely the heat source inlet and cooling water temperatures. Summarizing the data, the performance of the AD cycle can be expressed in terms of specific daily water production (SDWP) and the specific cooling power (SCP) for a

wide range of chilled-water inlet temperatures, typically ranging from 10 °C to 30 °C. The hot water and cooling water inlet temperatures are maintained at the rating conditions, namely at 85 °C and 30 °C respectively.

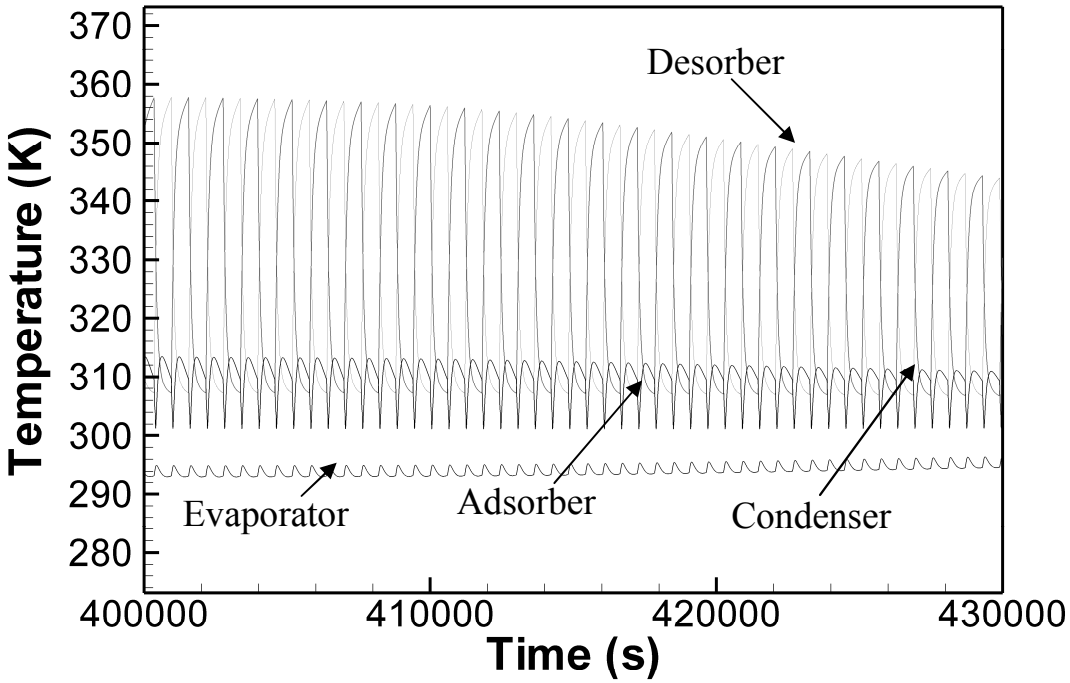

Fig. 5 The temperature profile of the solar-assisted adsorption desalination cum cooling cycle

	Temperature (°C)	Flow rate (kg/s)
Hot water inlet (desorber)	65-85	0.83
Cooling water inlet (adsorber)	29.5	0.83
Cooling water inlet (condenser)	29.5	2.00
Chilled water inlet (evaporator)	10-30	0.83
Mass of silica gel per bed (kg)	36	
Switching time (s)	40	
Evaporator (m^2)	7.5	
Condenser (m^2)	5.08	

Table 2. Operating conditions of the AD plant

The results show that both SDWP and SCP have a linear relationship with the chilled water inlet temperatures; that is increasing performance with higher chilled water inlet temperatures when the heat source temperature and cycle time are held constant. This is attributed to two factors: Firstly, an improvement in the boiling process at the evaporator and secondly, the increase in the pressurization effect of adsorbate onto the adsorbent caused by the higher evaporation temperature (hence P_{sat}). Figs. 8 and Fig. 9 depict the performance of the cycle for

two inlet chilled water temperatures i.e., 14 °C and 30 °C, subjected to varying hot water inlet temperatures. For the case of 30°C chilled water inlet temperature and optimized for potable water production, the daily average values of the SDWP and SCP are found to be 5.62m^3 and 45Rton per tonne of silica gel per day, respectively. Similarly, a lower SDWP of 2.1m^3 and SCP of 16.9 Rton per tonne of silica gel per day are expected when the chilled water inlet temperature is set at 14 °C. These simulation results indicate an excellent match for the adsorption cooling cum desalination cycles with the solar hot water collectors which have been designed for 270 m^2 and a water storage capacity (thermally-stratified design) of 12 m^3.

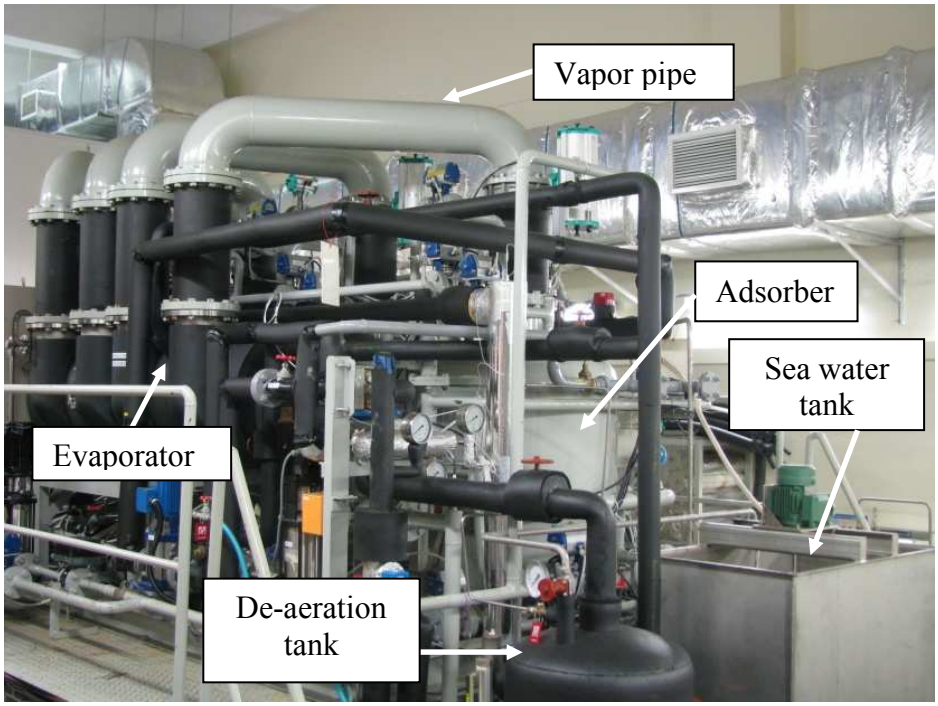

Fig. 6 The pilot adsorption desalination cum cooling plant in NUS

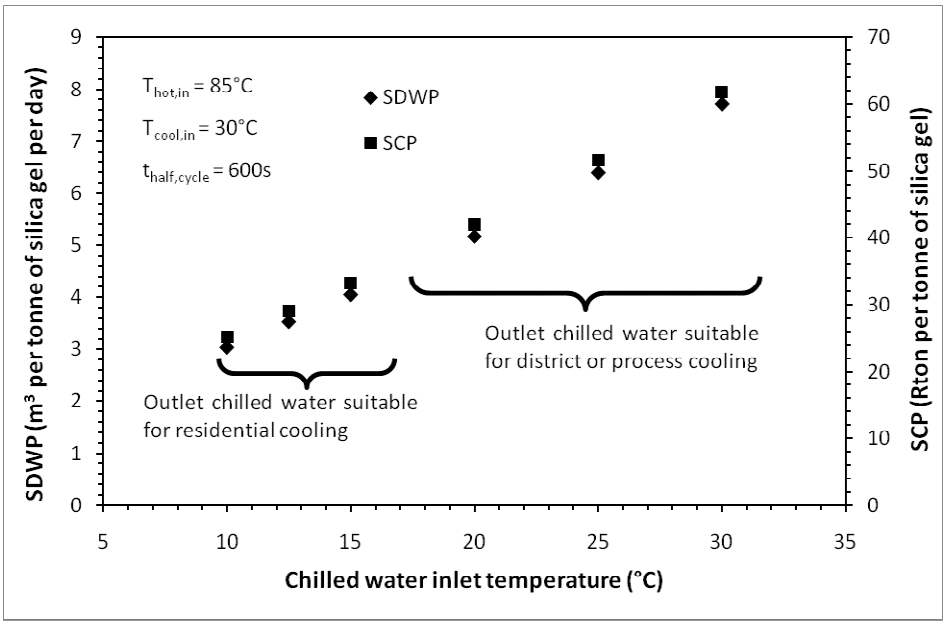

Fig. 7 SDWP and SCP of the AD cycle with assorted chilled water inlet temperatures suitable for residential cooling and process cooling applications

The key advantage of the AD cycle is the flexibility of operation over a wide range of heat source temperatures whilst the performances could improve with a lower coolant temperature supplied to the condenser. Being robust in the operational conditions, the cycle can be tailored to meet the requirements between the amount of cooling and the amount of desalted water needed by simply changing the temperature of evaporator. Should the AD operation is designed for more residential cooling, the predictions show that the cycle could produce a SCP of 32Rton and a SDWP of 4m^3 per day per tonne of silica gel when the outlet chilled water temperature spans from 7 °C to 10 °C. If more desalted water is desired from the condenser, the AD cycle operation could be adjusted to produce a SDWP and a SCP of 7.7 m^3 and 60 Rton per day per tonne of silica gel, respectively. For the latter operation, the cooling water from the evaporator would have to be raised higher, typically at 18 to 25 °C, a temperature range that is suited for process or district cooling.

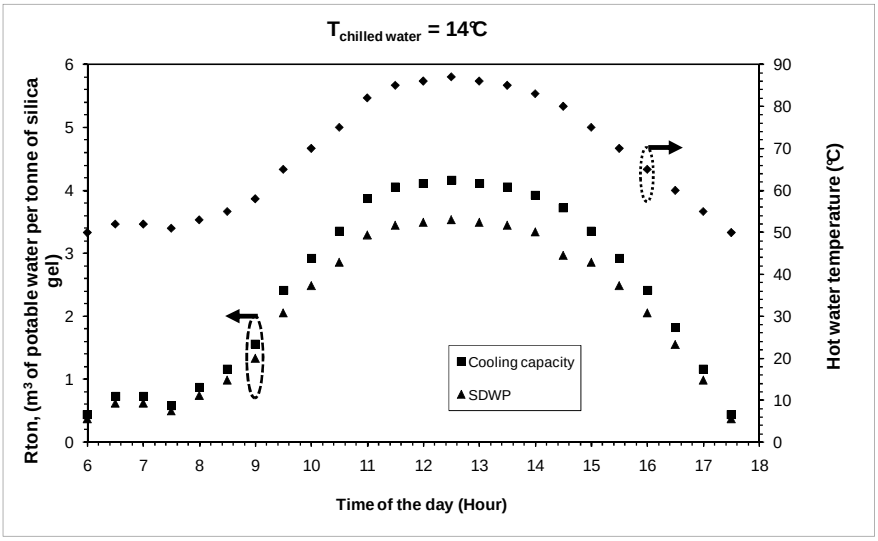

Fig. 8 Simulated results of the cooling capacity and the SDWP of the AD plant with hourly varying hot water temperature at chilled water inlet 14°C

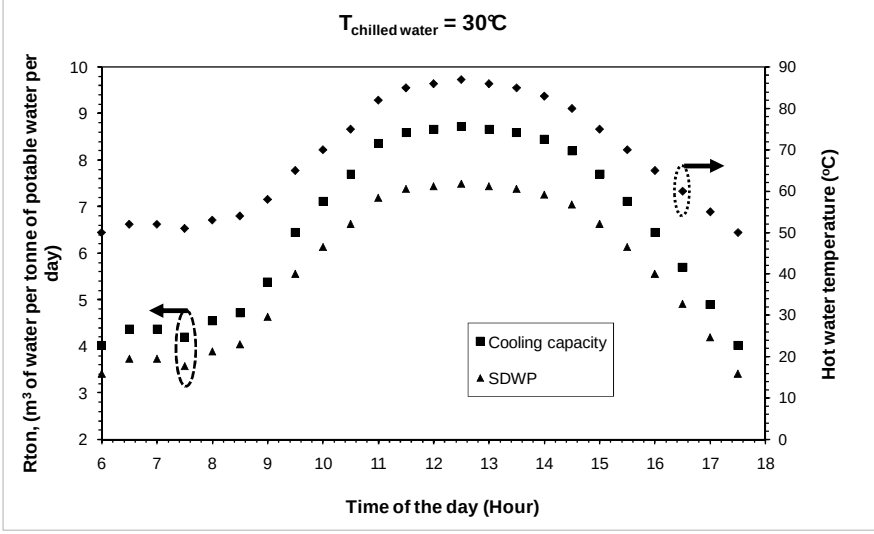

Fig. 9 Simulated results of the cooling capacity and the SDWP of the AD plant with hourly varying hot water temperature at chilled water inlet 30 °C

For a solar-driven adsorption cycle, the hot water temperatures from collectors are a function of daily insolation where the hot water temperature is expected to vary from 65 ˚C to 85 ˚C. The experimentally-measured performances of the AD plant are given in Fig. 10 and Fig. 11. It can be seen that the SDWP and the SCC of the adsorption cycle linearly increase with higher heat source temperature for every set of chilled water inlet temperature. It is also observed that both the SDWP and SCC of the adsorption cycle improve at higher chilled water temperatures with higher heat source temperatures.

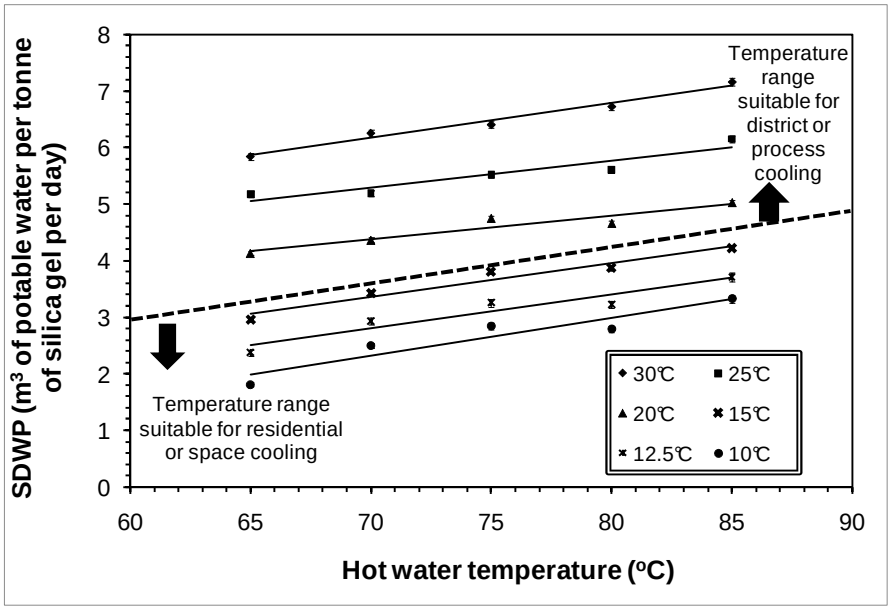

Fig. 10 SDWP of the adsorption cooling cum desalination cycle for different chilled water temperatures with assorted hot water inlet temperature

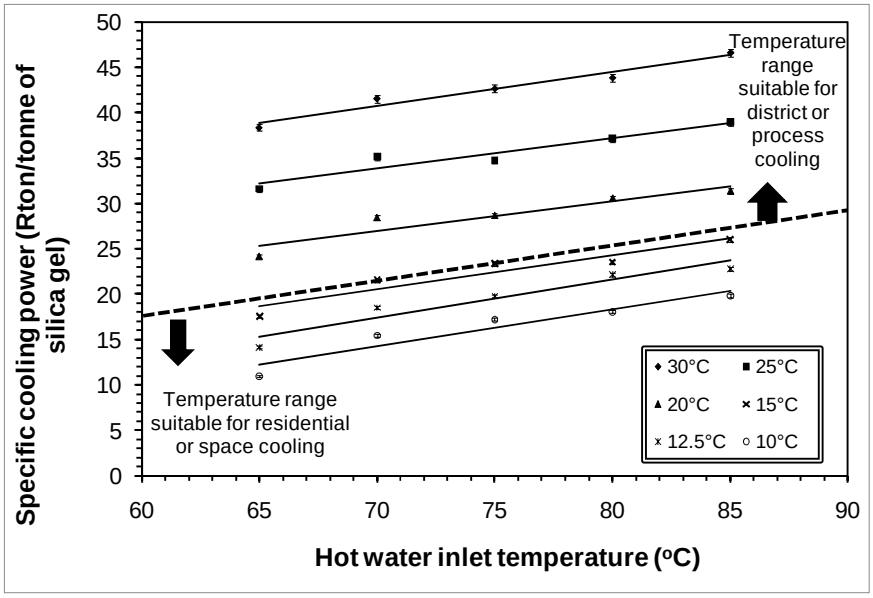

Fig. 11 SCP of the adsorption cooling cum desalination cycle for different chilled water temperatures with assorted hot water inlet temperature

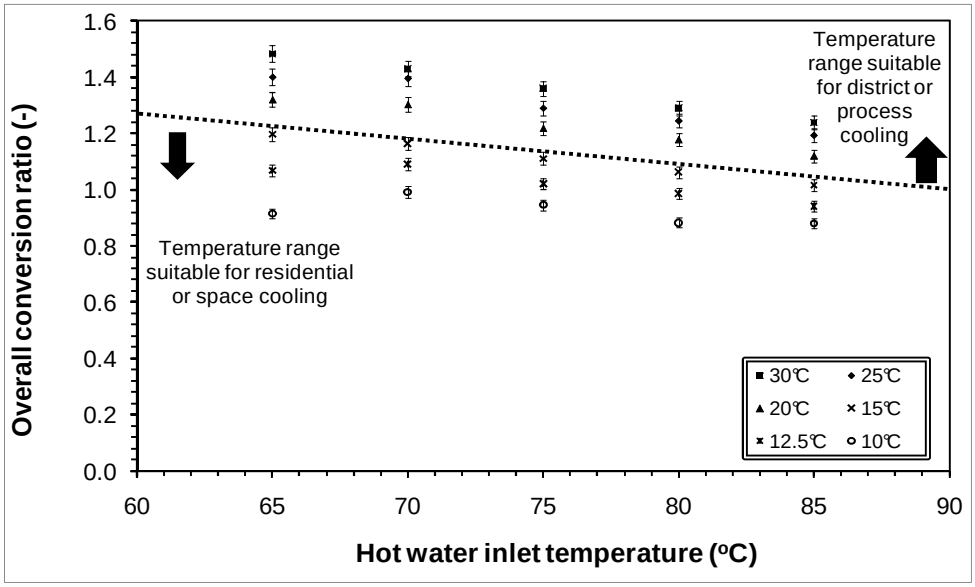

Fig. 12 Overall conversion ratio of the two-bed adsorption cycle for cooling and desalination

Fig. 12 describes the overall conversion ratio of the two-bed adsorption cycle for both air-conditioning and desalting applications at assorted hot water inlet and chilled water inlet temperatures. The results show that overall conversion of the Adsorption cycle decreases with increasing hot water temperature. The overall conversion ratio of the Adsorption cycle can be as high as 1.5 at 65 °C regeneration temperature. The results also show that the adsorption cycles can operate efficiently using solar energy.

Conclusions

The performance of an adsorption cooling cum desalination cycle has been investigated numerically and validated by experiments. The useful effects of the cycle i.e., cooling and potable water can be extracted when a single heat input at low temperature is supplied to the cycle. The results showed that the AD cycle produces a SCP of 32 Rton and a SDWP of 4m^3 per day per tonne of silica gel when the outlet chilled water temperature spans from 7 °C to 10 °C. At relatively higher chilled water temperature of 25 to 30 °C, the AD cycle produces a SDWP and a SCP of 7.7 m^3 and 60 Rton per day per tonne of silica gel, respectively. Being waste heat or solar energy driven, the electrical energy is used only for coolant circulation and hence, the payable energy of AD cycle is merely at 1.38kWh/m^3. With the simultaneous production of two useful effect i.e., cooling and potable water from the single heat input, the overall conversion ratio (OCR) of the AD cycle is observed to be about 1.4 at a hot water input of 65°C, making the waste-heat driven AD plant an excellent environment friendly machine.

References

[1] Jim S. Wallace and Peter J. Gregory, 2002, "Water resources and their use in food production systems", *Aquatic Science*, Vol. 64, pp. 363-375.

[2] www.waterfootprint.org

[3] Frenkel, V., (2004). "Desalination Methods, Technology and Economics" *Desalination Conference*, 2004, Santa Barbara, CA, USA.

[4] X. L. Wang and K.C. Ng, (2005), "Experimental investigation of an adsorption desalination plant using low-temperature waste heat", *Applied Thermal Engineering*, Vol. 25, pp. 2780-2789.

[5] Y. Al-Wazzan, F. Al-Modaf, (2001), "Seawater desalination in Kuwait using multistage flash evaporation technology- historical overview", *Desalination*, Vol. 134, pp. 257–267.
[6] Bart Van der Bruggen, Carlo Vandecasteele, (2002), "Distillation vs. membrane filtration: Overview of process evolutions in seawater desalination", *Desalination*, Vol. 143, pp. 207-218.
[7] S.A. Avlonitis, K. Kouroumbas, N. Vlachakis, (2003), "Energy consumption and membrane replacement cost for seawater RO desalination plants", *Desalination* Vol. 157 pp. 151-158.
[8] S.Al-Kharabsheh, D. Yogi Goswami, (2003), "Analysis of an innovative water desalination system using low-grade solar heat", *Desalination*, Vol. 156 pp. 323-332.
[9] Tamim Younos, Kimberly E. Tulou, (2005), "Overview of Desalination Techniques", *Journal of contemporary water research and education*, Vol. (132), pp 3-10.
[10] D.E. Weiss, (1996), "The role of ion-exchange desalination in municipal water supplies", *Desalination*, 1, 107-128.
[11] Roshdy A. Abdelrassoul, (1998), "Potential for economic solar desalination in the Middle East", *Renewable Energy*, Vol. 14, Nos. 1-4, pp. 345-349.
[12] Yosef Dreizin, (2006), "Ashkelon seawater desalination project - off-taker's self costs, supplied water costs, total costs and benefits", *Desalination*, Vol. 190 pp, 104–116.
[13] Ioannis C. Karagiannis, Petros G. Soldatos, (2008), "Water desalination cost literature: review and assessment", *Desalination*, Vol. 223 pp. 448–456.
[14] U. Atikol, Hikmet S. Aybar, (2005), "Estimation of water production cost in the feasibility analysis of RO systems", *Desalination*, Vol. 184 pp. 253–258.
[15] James E. Miller, (2003), "Review of Water Resources and Desalination Technologies".
[16] K. C. Ng, XL. Wang, LZ Gao, A. Chakraborty, B. B. Saha, S. Koyama, A. Akisawa and T. Kashiwagi, (2006), Apparatus and Method for Desalination, WO Patent number 121414.
[17] M T Bryk, R R Nigmatullin, (1994), "Membrane distillation", Russian Chemical Reviews, Vol. 63 (12) pp. 1047-1062.
[18] http://www.waterandclimatechange.eu/rainfall
[19] http://en.wikipedia.org/wiki/Precipitation_(meteorology)
[20] http://en.wikipedia.org/wiki/File:Breakdown_of_the_incoming_solar_energy.jpg
[21] Kyaw Thu, Chakraborty A, Saha B.B. and Ng K.C., (2010), "Life-Cycle Cost Analysis of Adsorption Cycles for Desalination", *Desalination and Water Treatment*, Vol. (20) pp. 1-10.
[22] J.E. Blank, G.F. Tusel, S. Nisan, (2007), "The real cost of desalted water and how to reduce it further", *Desalination*, Vol. 205, pp. 298–311.
[23] http://en.wikipedia.org/wiki/Adsorption
[24] Chi Tien, (1994), "Adsorption calculation and modeling", *Butterworh-Heinemann series in chemical engineering*, Boston.
[25] F. Rouquerol, J. Rouquerol and K. Sing (1999), "Adsorption by powers & porous solids, principles, methodology and applications", Boston.
[26] X.L. Wang, A. Chakraborty, K.C. Ng, B.B. Saha, (2007), "How heat and mass recovery strategies impact the performance of adsorption desalination plant: theory and experiments", *Heat Transfer Eng.*, Vol. 28 (2) pp. 147–153.
[27] A. Dąbrowski, (2001), "Adsorption - from theory to practice", *Advances in Colloid and Interface Science*, Vol. 93 pp. 135-224.
[28] K. C. Ng, H.T. Chua, C.Y. Chung, C.H. Loke, T. Kashiwagi, A. Akisawa, B.B. Saha, (2001), "Experimental investigation of the silica gel-water adsorption isotherm characteristics", *Applied Thermal Engineering*, Vol. 21, pp. 1631-1642.

[29] Ng, Kim Choon, Saha, Bidyut Baran, Chakraborty, Anutosh and Koyama, Shigeru, (2008), "Adsorption Desalination Quenches Global Thirst", *Heat Transfer Engineering*, Vol. 29 (10), pp. 845-848.
[30] Duffie, J.A., Beckman, W.A., (1991). "Solar Engineering of Thermal Processes", John Wiley & Sons Inc., New York.
[31] Spencer, J.W., (1971), "Fourier series representation of the position of the sun". Search 2, 172–177.
[32] Collares-Pereira, M., Rabl, A., (1979), "The average distribution of solar radiation-correlations between diffuse and hemispherical and between daily and hourly insolation values", *Solar Energy*, Vol. 22, pp. 155–164.
[33] Liu, B.Y.H., Jordan, R.C., (1960), "The interrelationship and characteristic distribution of direct, diffuse and total solar radiation", *Solar Energy*, Vol. 4, pp. 1-19.
[34] Hay, J.E., Davies, J.A., (1980), "Calculation of the solar radiation incident on an inclined surface", *Proceedings of the First Canadian Solar Radiation Data Workshop*, pp. 59–72.
[35] Temps, R.C., Coulson, K.L., (1977), "Solar radiation incident upon slopes of different orientations", *Solar Energy*, Vol. 19, pp. 179–184.
[36] Klucher, T.M., (1979), "Evaluation of models to predict insolation on tilted surfaces", *Solar Energy*, Vol. 23, pp. 111–114.
[37] Rabl, A., (1985), "Active Solar Collectors and their Applications", Oxford University Press, Oxford.
[38] McIntire, W.R., (1982), "Factored approximations for biaxial incident angle modifiers", *Solar Energy*, Vol. 29, pp. 315–322.
[39] Anutosh Chakraborty, Bidyut Baran Saha, Ibrahim I. El-Sharkawy, Shigeu Koyoma, Kandadai Srinivasan and Kim Choon Ng, (2009), "Theory and experimental validation on isosteric heat of adsorption for an adsorbent+adsorbate system", *High Temperatures-High Pressures*, Vol. 37, pp. 109-117.
[40] Anutosh Chakraborty, Bidyut Baran Saha, Kim Choon Ng, Shigeu Koyoma and Kandadai Srinivasan, (2009), Theoretical Insight of Physical Adsorption for a Single-Component Adsorbent+Adsorbate System: I. Thermodynamic Property Surfaces, *Langmuir*, Vol. 25 (4), 2204-2211.